

1 **Stability and heterogeneity in the anti-microbiota reactivity of human milk-derived**  
2 **Immunoglobulin A**

3

4 Chelseá B. Johnson-Hence<sup>1,2</sup>, Kathyayini P. Gopalakrishna<sup>1</sup>, Darren Bodkin<sup>1</sup>, Kara E.  
5 Coffey<sup>1,3</sup>, Ansen H.P. Burr<sup>1,4</sup>, Syed Rahman<sup>4,5</sup>, Ali T. Rai<sup>1</sup>, Darryl A. Abbott<sup>1</sup>, Yelissa A.  
6 Sosa<sup>1</sup>, Justin T. Tometich<sup>1</sup>, Jishnu Das<sup>4,5</sup>, Timothy W. Hand<sup>1,4\*</sup>

7

8 <sup>1</sup>R.K. Mellon Institute for Pediatric Research, Pediatrics Department, Infectious Disease  
9 Section, UPMC Children's Hospital of Pittsburgh, University of Pittsburgh School of  
10 Medicine, Pittsburgh PA, 15224

11 <sup>2</sup>Department of Pediatrics, Division of Neonatal-Perinatal Medicine, University of Texas  
12 Southwestern Medical Center

13 <sup>3</sup>Department of Pediatrics, Division of Allergy and Immunology, University of Pittsburgh  
14 School of Medicine

15 <sup>4</sup>Department of Immunology, University of Pittsburgh School of Medicine

16 <sup>5</sup>Center for Systems Immunology, University of Pittsburgh School of Medicine

17

18 \*Corresponding author and lead contact: [timothy.hand@chp.edu](mailto:timothy.hand@chp.edu)

19

20 **Summary:** We analyze the ability of breast milk-derived Immunoglobulin A (IgA)  
21 antibodies to bind the infant intestinal microbiota. We discover that each mother  
22 secretes into their breast milk a distinct set of IgA antibodies that are stably maintained  
23 over time.

24  
25 **Abstract:** Immunoglobulin A (IgA) is secreted into breast milk and is critical to both  
26 protecting against enteric pathogens and shaping the infant intestinal microbiota. The  
27 efficacy of breast milk-derived maternal IgA (BrmlgA) is dependent upon its specificity,  
28 however heterogeneity in BrmlgA binding ability to the infant microbiota is not known.  
29 Using a flow cytometric array, we analyzed the reactivity of BrmlgA against bacteria  
30 common to the infant microbiota and discovered substantial heterogeneity between all  
31 donors, independent of preterm or term delivery. We also observed intra-donor  
32 variability in the BrmlgA response to closely related bacterial isolates. Conversely,  
33 longitudinal analysis showed that the anti-bacterial BrmlgA reactivity was relatively  
34 stable through time, even between sequential infants, indicating that mammary gland  
35 IgA responses are durable. Together, our study demonstrates that the anti-bacterial  
36 BrmlgA reactivity displays inter-individual heterogeneity but intra-individual stability.  
37 These findings have important implications for how breast milk shapes the development  
38 of the infant microbiota and protects against Necrotizing Enterocolitis.

39

40 **Introduction:**

41 Breast milk is acknowledged by the World Health Organization and American Academy  
42 of Pediatrics as the best source of nutrition for infants (Sobti et al., 2002). Breast milk  
43 contains multiple bioactive components, including antibodies, that both prevent infection  
44 and aid in the proper installation of the infant microbiota (Gopalakrishna and Hand,  
45 2020; Le Doare et al., 2018; Walker and Iyengar, 2015). IgA, IgG and IgM antibodies  
46 are all found in breast milk, but IgA is dominant, making up over 90% of the antibody  
47 secreted in the mammary gland. One reason for this is that during pregnancy, IgA-  
48 producing B cells are compelled to travel from the intestine to the mammary gland,  
49 indicating that IgA secreted into milk is an effort to transfer maternal mucosal immunity  
50 to the infant (Lindner et al., 2015; Wilson and Butcher, 2004). During B cell production,  
51 IgA is often dimerized by the J-chain which promotes binding and transcytosis of IgA by  
52 the polymeric glycoprotein Ig receptor (pIgR) that upon secretion remains bound to IgA  
53 as 'Secretory Factor' (SF) (Hand and Reboldi, 2021). SF-bound of 'secretory; IgA  
54 (SIgA) is protected against proteolytic cleavage in the intestine, substantially increasing  
55 the half-life and functionality of IgA half-life and functionality of IgA at mucosal surfaces  
56 (Johansen and Kaetzel, 2011). The majority of IgA secreted into breast milk is SIgA  
57 (Rogier et al., 2014).

58

59 In addition to protecting against infection (Gopalakrishna and Hand, 2020), SIgA is  
60 important in shaping the development of the infant microbiota (Planer et al., 2016;  
61 Rogier et al., 2014). In breast fed infants, milk is the predominant source of IgA in the  
62 first month of life and in mice, lack of maternal IgA affects the development of the

63 microbiota (Gopalakrishna et al., 2019; Mirpuri et al., 2014; Rognum et al., 1992). Infant  
64 formula, which lacks all immunoglobulins, is also associated with alterations in the infant  
65 microbiota and increased rates of short and long-term diseases (Dixon, 2015; Oddy,  
66 2017). Preterm infants are particularly susceptible to diseases related to improper  
67 regulation of colonization by microbiota, like necrotizing enterocolitis (NEC) (Bode,  
68 2018; Cortez et al., 2018; Neu and Walker, 2011; Nino et al., 2016; Warner and Tarr,  
69 2016). The incidence of NEC is significantly increased in formula-fed preterm infants  
70 and the promotion of milk feeding in these children has reduced the incidence of this  
71 disease (Neu and Walker, 2011; Nino et al., 2016). In a cohort of milk-fed preterm  
72 infants, we have demonstrated that in the days directly preceding the development of  
73 NEC, there is a substantial reduction in the fraction of intestinal bacteria bound by  
74 breast milk-derived IgA, that is not typically observed in infants who do not develop  
75 disease (Gopalakrishna et al., 2019). The majority of IgA ‘unbound’ bacteria in preterm  
76 NEC infants come from one family: *Enterobacteriaceae*, which has previously been  
77 associated with the disease (Gopalakrishna et al., 2019; Pammi et al., 2017). Changes  
78 to IgA binding of the infant microbiota could either be caused by a shift in the  
79 composition of the microbiota or the anti-bacterial IgA reactivity of the breast milk. The  
80 level of heterogeneity in milk-derived IgA between individuals and over time within one  
81 mother is not well understood, but due to their intestinal origin (Lindner et al., 2015), the  
82 anti-bacterial reactivity of human mammary gland-resident IgA-producing B cells is likely  
83 to be highly individualized.

84

85 To measure the milk-derived anti-bacterial IgA response we have developed a flow  
86 cytometric array that allows us to define the ability of antibodies to bind the surface of  
87 different bacterial isolates. Using this array, we have identified significant heterogeneity  
88 between different donors in the binding of bacterial isolates by milk-derived IgA. We  
89 also observed isolate level variation in IgA binding, within donor samples, to closely  
90 related taxa of *E. coli* and other species. In contrast to the inter-individual heterogeneity,  
91 hierarchical clustering and Principal Component Analysis (PCA) of longitudinally  
92 collected samples showed consistent clustering within donors, indicating that the anti-  
93 bacterial IgA reactivity of an individual is stable over the course of one infant. Analysis  
94 of milk samples collected over sequential siblings also revealed stability in anti-bacterial  
95 IgA reactivity, indicating that the B cells that secrete IgA into breast milk may be  
96 maintained long-term. Finally, we demonstrate that Holder pasteurization, which is  
97 commonly used to sterilize human donor milk, globally reduces bacterial binding by IgA.  
98 Together our data indicates that the anti-bacterial reactivity of milk-derived IgA is  
99 heterogeneous between individuals but also surprisingly stable, even over infants  
100 separated by years of time. The temporal stability of breast milk-derived IgA reveals a  
101 potential weakness of vertical antibody transmission, where maternal antibody  
102 responses are uncoupled from infant intestinal bacterial colonization, potentially limiting  
103 BrmIgA's protective effects against infection and NEC (Gopalakrishna et al., 2019).  
104

105 **Results:**

106 **Determining anti-bacterial IgA reactivity of breast milk using a flow cytometric**  
107 **array.**

108 Anti-bacterial IgA is predominantly specific to surface antigens and bacterial staining  
109 techniques that use bacterial lysates are complicated by irrelevant antibody cross-  
110 reactivity against cytoplasmic proteins and nucleic acids (Slack et al., 2009). Therefore,  
111 we modified an approach described by Slack and colleagues to measure anti-bacterial  
112 IgA specificity of breast milk antibodies by flow cytometry (Moor et al., 2016; Slack et  
113 al., 2009). To negate non-specific signals associated with the non-IgA components of  
114 breast milk we isolated SIgA via passage over a streptococcal Peptide M column. LDS-  
115 PAGE under reducing conditions of the Peptide M bound fraction revealed bands  
116 roughly corresponding in size to Secretory Factor (~80kDa), IgA Heavy Chain (~60kDa)  
117 and Light Chain (~30kDa) (**Fig. S1A**)(Sandin et al., 2002). J-chain (15kDa) is known to  
118 migrate slowly under LDS-PAGE electrophoresis and is the faint band running slightly  
119 below the Light chain at ~25kDa (**Fig. S1A**) (Zikan et al., 1985). We confirmed by  
120 Western blot that each of the four components of SIgA were enriched in the Peptide M  
121 bound fraction (**Fig. S1B**). To determine the specificity of an IgA enriched breast milk  
122 sample for bacterial surface antigens we incubated purified IgA samples on bacterial  
123 isolates individually arrayed on a 96 well plate (**Fig. 1A**). Prior to flow cytometric  
124 analysis samples were normalized to rough protein content (280nm Absorbance), which  
125 corresponds well to the concentration of IgA measured by ELISA (**Fig. S1C**). After  
126 incubation with breast milk-derived IgA, bacteria are stained with a mixture of Syto BC  
127 and fluorescently-labelled anti-human IgA. Syto BC is a mixture of bacterial cell wall

128 permeable dyes that allow us to discriminate bacteria from similarly sized debris on the  
129 flow cytometer (**Fig. 1B**). Syto BC<sup>+</sup> bacteria can then be assayed for binding by breast  
130 milk-derived IgA by assessing the relative fluorescence normalized to a background  
131 control of the same bacteria stained only with anti-human IgA secondary antibody (**Fig.**  
132 **1C**). Analysis of a dilution series of purified IgA samples revealed that the concentration  
133 of SIgA used to test bacterial binding (0.1mg/mL) was saturating for the bacteria tested  
134 and thus was used as a standard concentration for all further experiments (**Fig. S1D**).  
135 To control for non-specific binding of BrmIgA by bacteria we tested a monoclonal  
136 antibody specific to HIV against our array and found only very minimal binding,  
137 indicating that our array is measuring anti-bacterial IgA responses (**Fig. 1C**)(Yu et al.,  
138 2013). Further, binding of BrmIgA to a soil bacterium *Bradyrhizobium japonicum*,  
139 demonstrated marginal signal, indicating that the breast milk-derived IgA response is  
140 focused on bacterial taxa that commonly colonize humans (**Fig. 1D**)(Haas et al., 2011).

141

#### 142 **Heterogeneity in the breast milk-derived anti-bacterial IgA reactivity.**

143 After delivery the infant microbiota goes through three main stages (Reyman et al.,  
144 2019). First, the infant intestine becomes colonized by common facultative anaerobic  
145 bacteria such as *Enterobacteriaceae* and *Enterococcaceae*. Within the next four weeks  
146 these bacteria will be supplanted as the dominant taxa by *Bifidobacteria*, which use  
147 Human Milk Oligosaccharides as a food source. Six months later, approximately  
148 coinciding with the introduction of solid food, there is another switch towards anaerobic  
149 *Firmicutes* and *Bacteroidetes* that assist with the digestion of complex carbohydrates.  
150 BrmIgA likely contributes to shaping microbiota colonization at all of these stages, but is

151 particularly important for controlling the early bacterial colonizers that comprise the first  
152 stage when infants don't make their own IgA (Gopalakrishna et al., 2019; Koch et al.,  
153 2016; Mirpuri et al., 2014; Rognum et al., 1992). Indeed, mouse pups fed by dams that  
154 lack IgA production or secretion are colonized with facultative anaerobes such as  
155 *Enterobacteriaceae* and *Pastereurellaceae* longer than IgA-secreting controls (Mirpuri et  
156 al., 2014; Rogier et al., 2014). Regulation of early colonizing bacteria is especially  
157 relevant to preterm infants where increased *Enterobacteriaceae* and in particular IgA-  
158 free *Enterobacteriaceae* is associated with the development of Necrotizing Enterocolitis  
159 (NEC) (Gopalakrishna et al., 2019; Pammi et al., 2017). Thus, when designing the  
160 bacterial array for analyzing the anti-bacterial reactivity of breast milk-derived IgA, we  
161 focused on facultative anaerobes, such as *Enterobacteriaceae*, that dominate early  
162 infant bacterial colonization. Our array contained 36 individually grown and plated  
163 bacterial isolates from 13 different genera that represent the major taxa commonly  
164 found in the intestine of preterm infants. All donor samples were normalized for the input  
165 concentration of IgA. Analysis of the anti-bacterial IgA responses from 33 donors  
166 revealed a substantial amount of heterogeneity, with no two donors being identical (**Fig.**  
167 **2A**). Thus, individualized differences in the IgA<sup>+</sup> B cell population of the intestine driven  
168 by distinct infection and microbiota experiences likely lead to similar heterogeneity in the  
169 breast milk (Bunker et al., 2017; Hapfelmeier et al., 2010; Lindner et al., 2015; Zhang et  
170 al., 2017). Comparative analysis of the normalized magnitude of BrmIgA across all  
171 bacterial isolates revealed that rather than particular donors making universally strong  
172 or weak responses against all bacterial isolates, there was substantial heterogeneity in  
173 donor binding from bacterial isolate to isolate (**Fig. 2A-B**). The magnitude of IgA binding



174 to different bacterial isolates was also evenly distributed, where normalized IgA binding  
175 for most isolates shared a similar standard deviation (~1 to 5), though some donors had  
176 exceptionally strong binding to different *Staphylococcus* isolates (**Fig. 2B**). Conversely,  
177 some bacterial isolates (*Serratia marcescens* 855, *Proteus mirabilis*, *Lactobacillus*  
178 *casei*) were bound by BrmIgA from few donors (**Fig. 2B**). The heterogeneity of anti-  
179 bacterial IgA reactivity was also demonstrated by comparison of BrmIgA responses to  
180 related isolates of *E. coli* where the magnitude of response to each isolate of *E. coli* was  
181 highly individual to the donor and could vary more than 5-fold (**Fig. 2C**). Species and  
182 isolate level heterogeneity was also evident in responses against *Staphylococcus*,  
183 *Serratia*, *Klebsiella* and *Enterococcus* (**Fig. 2A-B**). Despite this evident heterogeneity,  
184 we wanted to measure whether any of the anti-bacterial IgA responses were correlated,  
185 such that response to one bacterium would be predictive of another. To test this  
186 possibility, we used correlation network analyses to identify statistically significant  
187 pairwise relationships between different bacteria isolates (Ackerman et al., 2018;  
188 Suscovich et al., 2020). These analyses focus on the most significant pairwise  
189 correlations of IgA binding profiles across the different bacterial isolates and revealed  
190 substantial interconnection and correlated responses specific to *Enterobacteriaceae*  
191 isolates (**Fig. 2D**). This finding is consistent with a previous discovery of a high degree  
192 of *Enterobacteriaceae* cross-reactivity in blood-derived human IgA clones, due to  
193 reactivity to shared surface molecules, such as lipopolysaccharide (Rollenske et al.,  
194 2018). To gain a more comprehensive understanding of global relationships in IgA  
195 binding profiles across bacterial isolates, we visualized all pairwise correlations in a  
196 heatmap (**Fig. 2E**). The correlation heatmap showed two clear blocks – one composed

197 entirely of *Enterobacteriaceae* involving highly correlated profiles, and the other  
198 involving relatively uncorrelated profiles. There were no strong correlations discovered  
199 amongst Gram Positive bacteria, even when comparing isolates of the same bacterial  
200 species (**Fig. 2D-E**). Taken together, our data indicates that even though anti-  
201 *Enterobacteriaceae* IgA responses are common and broad, the breast milk-derived anti-  
202 bacterial BrmIgA response is quite heterogeneous from person to person.  
203 Heterogeneity in anti-bacterial IgA may be important to newborns where IgA binding (or  
204 lack thereof) to infant intestinal bacteria can regulate bacterial colonization.

205

206 **Heterogeneity in the breast milk-derived anti-bacterial IgA reactivity from donors**  
207 **who delivered preterm infants.**

208 It is not known when during pregnancy-induced mammary gland (MG) development that  
209 B cells traffic from the intestine to the MG. In mice it predominantly occurs late in  
210 gestation or even after delivery, whereas in pigs it occurs maximally in the 2<sup>nd</sup> trimester  
211 (Langel et al., 2019; Roux et al., 1977). If B cell traffic to the MG during the 3<sup>rd</sup> trimester  
212 is required for optimal breast milk IgA secretion in humans, preterm delivery, which  
213 often occurs at the transition between the 2<sup>nd</sup> and 3<sup>rd</sup> trimesters, may affect the level  
214 and specificity of breast milk-derived IgA. Comparison of the concentration of IgA from  
215 milk samples derived from preterm mothers (Gestational age 24-35 weeks) and term  
216 (>37 weeks) samples revealed no significant difference (**Fig. 3A**). Further, BrmIgA  
217 isolated from preterm milk samples phenocopied term milk samples with regard to  
218 heterogeneity within the anti-bacterial reactivity (**Fig. 3B-C**). Finally, PCA could not  
219 separate term and preterm samples on the basis of the anti-bacterial binding reactivity,

220 indicating that, by the metrics of IgA concentration in the milk and anti-bacterial binding,  
221 preterm and term BrmIgA are effectively indistinguishable (**Fig. 3D**).

222

### 223 **Temporal stability of anti-bacterial maternal IgA reactivity within one** 224 **childbirth/infant.**

225 The concentration of all proteins, including BrmIgA, is highest in colostrum and then  
226 recedes to a stable point after the transition into mature milk, but whether this shift is  
227 associated with changes in the anti-bacterial reactivity of BrmIgA is not known. For  
228 example, whether B cells traffic in and out of the mammary gland during lactation, thus  
229 changing BrmIgA reactivity, is not well understood. We tested the stability of the anti-  
230 bacterial BrmIgA reactivity of various milk donors throughout their lactation periods,  
231 testing samples from each of the stages (colostrum, transitional, mature). All samples  
232 were normalized for the input concentration of IgA, which is critical to account for the  
233 increased level of IgA in colostrum. Hierarchical clustering of the longitudinal samples  
234 from the seven donors revealed that in general, samples captured from the same donor  
235 over long periods of time generally clustered together, indicating that they resemble  
236 other samples from the same donor more than they resemble samples from another  
237 donor (**Fig. 4A**). Longitudinal comparison of the magnitude of the IgA response against  
238 each bacterial isolate also revealed no generalizable trend towards increased or  
239 decreased anti-bacterial IgA binding as samples transitioned from colostrum/  
240 transitional milk to mature milk (**Fig. S2**). Graphical depiction of the magnitude of the  
241 response against each bacterial isolate also revealed ‘clustering’ of samples within  
242 donor groups (**Fig. 4B**; each donor is one color). Finally, PCA analysis demonstrated

243 that the collections of samples from different donors generally formed distinct clusters  
244 (**Fig. 4C and D**). Similar to data captured from individual mothers of term and preterm  
245 infants (**Fig. 2 and 3**), longitudinal samples show significant heterogeneity between  
246 donors. Thus, while the anti-bacterial BrmIgA reactivity of each donor is distinct, within  
247 each mother, the anti-bacterial antibodies and perhaps mammary gland resident B cells  
248 are stable.

249

### 250 **Relative stability of the breast milk anti-bacterial IgA through siblings**

251 During pregnancy, B cells are induced to traffic from the small intestine and Peyer's  
252 Patches to the mammary gland (Lindner et al., 2015; Ramanan et al., 2020; Wilson and  
253 Butcher, 2004). In contrast to vaccine-specific B cells, microbiota-specific plasma B  
254 cells in the small intestine are believed to be replaced at a high rate and thus we  
255 hypothesized that the anti-bacterial reactivity of BrmIgA might shift substantially  
256 between sequential childbirths (Bemark et al., 2016; Hapfelmeier et al., 2010;  
257 Landsverk et al., 2017). To test this hypothesis, we acquired samples from a single  
258 donor over sequential infants and analyzed for changes in their anti-bacterial reactivity.  
259 Hierarchical clustering of these samples revealed that they clustered together and that  
260 samples captured after the 2<sup>nd</sup> childbirth were more similar to the previous sample from  
261 the same individual than any other donor (**Fig. 5A**). PCA analysis confirmed the  
262 similarity of samples from sequential infants (**Fig. 5B**; comparison of the location of the  
263 same colored circles and triangles). There were individualized changes in IgA binding to  
264 different bacterial isolates between infants, but no generalizable bacterial isolate-  
265 specific trends were detected in the dataset between siblings (**Fig. 5A**). However,

266 paired analysis of each multi-infant couplet comparing the mean change in anti-IgA  
267 binding across all of the isolates revealed that for the majority of donors anti-bacterial  
268 binding increased (6/10; upward pointing triangles) or stayed the same (2/10; circles)  
269 from the 1<sup>st</sup> childbirth to subsequent childbirths (**Fig. 5C and Fig. S3**). Thus, we have  
270 observed that even between childbirths there is some stability in the anti-bacterial  
271 reactivity, implying either that B cells can permanently reside in the mammary gland  
272 outside of periods of lactation, or alternatively that the same or similar B cells are  
273 trafficking from mucosal sites during each pregnancy.

274

### 275 **Holder Pasteurization reduces the bacterial binding properties of breast milk-** 276 **derived IgA**

277 Increasingly, donor milk is being used as a substitute for Mother's Own Milk (MOM)  
278 (Haiden and Ziegler, 2016). Donor milk has been shown to provide some of the benefits  
279 of MOM, including a reduction in the incidence of NEC, compared to formula-fed infants  
280 (Boyd et al., 2007; Canizo Vazquez et al., 2019; Miller et al., 2018; Quigley et al., 2018).  
281 To prevent the transfer of potentially pathogenic bacteria, donor milk is pasteurized by  
282 the Holder method (62.5°C for 30 minutes). An unfortunate consequence of Holder  
283 pasteurization is the denaturation of proteins and a reduction in the function of many of  
284 the immunological components of breast milk (Adhisivam et al., 2018). Secretory IgA is  
285 particularly stable, but it has been estimated that ~13-62% of IgA is lost by Holder  
286 Pasteurization (Adhisivam et al., 2018; Lima et al., 2017; Peila et al., 2016). Here we  
287 split four donor samples in two and compared IgA concentrations and anti-bacterial IgA  
288 binding between raw control and Holder pasteurized samples. ELISA for the

289 concentration of IgA before and after pasteurization revealed a 2-3-fold drop in the  
290 concentration of IgA, consistent with published literature (**Fig. 6A**). Critically, after  
291 normalizing for protein content between paired pasteurized and control samples we still  
292 detected an additional reduction in BrmIgA anti-bacterial binding responses to most  
293 isolates assayed (**Fig. 6B**). Thus, Holder pasteurization reduces both the amount and  
294 anti-bacterial binding capability of breast milk-derived IgA.  
295

## 296 **Discussion**

297 Here we demonstrate that the anti-bacterial reactivity of IgA in breast milk is  
298 heterogeneous between individuals but stable over time, both within one infant and over  
299 multiple childbirths. We did not find any appreciable difference in IgA content or  
300 functionality between preterm and term mothers. Additionally, we found that Holder  
301 pasteurization generally reduces the ability of breast milk-derived BrmIgA to bind  
302 bacteria, regardless of the identity of the bacteria.

303

304 A limitation of our study is the lack of obligate anaerobic bacteria within our flow  
305 cytometric array. We focused upon the facultative anaerobes that dominate the early  
306 colonization period of the infant because there is evidence that this is a critical time  
307 when BrmIgA is necessary to control microbiota colonization (Gopalakrishna et al.,  
308 2019; Mirpuri et al., 2014; Rognum et al., 1992), and that failure to control facultative  
309 anaerobes (*Enterobacteriaceae*, *Enterococcaceae*, *Streptococcaceae* etc.) is related to  
310 the development of NEC and other infant diseases (Flannery et al., 2021; Lin et al.,  
311 2022; Olm et al., 2019; Warner and Tarr, 2016). Obligate anaerobes are also  
312 problematic substrates for our flow cytometric array, which requires multiple staining  
313 and centrifugation steps difficult to perform in an anaerobic chamber and we are  
314 concerned that exposure to oxygen might kill or modify the bacteria leading to  
315 misleading results.

316

317 It is not surprising that each donor in our study possessed a distinct collection of anti-  
318 bacterial antibodies as this is likely the result of distinct life histories with regard to

319 gastrointestinal infection and microbiota composition. Interestingly, we observed  
320 differences in the ability of individual donors to bind different isolates from the same  
321 species of bacteria. T cell-dependent IgA producing B cells are more likely to be  
322 targeted to bacterial surface proteins and less likely to be specific to repetitive structures  
323 on the bacteria's surface. Thus, our findings support the hypothesis, derived from  
324 experiments in mice, that the majority of mammary gland resident IgA-producing B cells  
325 are the product of T cell-dependent activation (Bunker et al., 2017). We hypothesize  
326 that the specificity of milk-derived IgA is skewed towards heterogeneous surface  
327 proteins that differ between isolates of the same species, contributing to isolate level  
328 heterogeneity in IgA binding. Non-proteinaceous antigens (such as LPS) are also  
329 incredibly diverse in different bacterial isolates and are likely to contribute to the  
330 heterogeneity of breast milk-derived anti-bacterial reactivity. Conversely using network  
331 analyses, we do see some evidence of correlation between breast milk-derived anti-  
332 bacterial IgA responses directed against various *Enterobacteriaceae* family bacteria.  
333 Perhaps *Enterobacteriaceae* share surface structures to a greater degree than other  
334 bacteria we tested in our array, increasing the likelihood of IgA cross-reactivity  
335 (Rollenske et al., 2018). It is possible that if we expanded the numbers of Gram Positive  
336 bacteria in the array that we would see more evidence of cross-reactivity, but we should  
337 note that amongst six isolates of *Staphylococcaceae* we observed no correlation in  
338 antibody responses.

339

340 In contrast to the heterogeneity that we observed between donors, we observed little  
341 heterogeneity in samples captured at different stages (from the same donor). This



342 indicates that B cells may become established in the developing mammary gland and  
343 do not turn over to a substantial degree over the course of one infant. Indeed, the same  
344 B cell clones can be identified in breast milk samples over multiple timepoints (Bondt et  
345 al., 2021). This is important and underscores a key limitation of vertical antibody  
346 transmission into infants, which is that the maternal IgA response is physically separate  
347 from the target of its protective effect (infant's intestine) and thus it does not respond to  
348 either bacterial or viral colonization of the infant. This is highly relevant to diseases  
349 common to preterm infants such as NEC and sepsis, where IgA present in breast milk  
350 may help prevent invasion by the nascent microbiota (Gopalakrishna et al., 2019).  
351 However, our results indicate that in some circumstances BrmIgA might not bind all  
352 infant intestinal bacteria and these 'holes' in anti-bacterial reactivity would persist  
353 throughout the breast feeding period, allowing unbound bacteria to proliferate and  
354 colonize more effectively. Previously, we observed a drop in IgA binding of  
355 *Enterobacteriaceae* that proceed the development of NEC (Gopalakrishna et al., 2019)  
356 and our new data implies that this observation is due a shift in the microbiota to escape  
357 maternal IgA and not change in the anti-bacterial IgA reactivity of the milk. Thus, for  
358 particularly at-risk preterm infants, it may be helpful to supplement breast milk with IgA  
359 known to bind the bacteria best associated to diseases like NEC.

360

361 We also observed that the anti-bacterial reactivity of BrmIgA was stable within one  
362 donor over multiple childbirths. This is somewhat surprising because the microbiota-  
363 specific B cells that populate the mammary gland traffic from the intestine and IgA  
364 producing B cells in the intestine are believed to turn over at a high rate (Hapfelmeier et

365 al., 2010). Therefore, each pregnancy should lead to the deposition of new B cells and  
366 shifts in the anti-bacterial reactivity of BrmIgA. Our results demonstrated that BrmIgA  
367 reactivity from samples collected from one donor over several years and different  
368 infants looked more similar to each other than to any other donor, implying that either  
369 intestinal IgA-producing B cells are more stable than previously thought (Bemark et al.,  
370 2016), or that once established in the breast tissue, B cells can remain, even after  
371 lactation has been completed. In support of this idea, the majority of donors saw their  
372 responses either stay the same or improve in subsequent pregnancies. Whether B cells  
373 reside in mammary glands outside of the period of lactation and can be re-activated  
374 upon a subsequent pregnancy is testable in rodent models.

375

376 Feeding preterm infants human milk is well described to reduce the incidence of NEC  
377 compared to infant formula. Often for preterm infants, the mother's milk production is  
378 insufficient and thus it is becoming more common to supplement the infant diet with  
379 pasteurized donor milk. Whether donor milk is as effective as Mother's Own Milk (MOM)  
380 for protecting against NEC has not been conclusively determined (Quigley et al., 2018).  
381 Here we demonstrate that pasteurization reduces the both the amount of IgA in breast  
382 milk and the ability of BrmIgA to bind bacteria. Thus, if IgA is important for the  
383 effectiveness of donor milk in reducing NEC, one might suspect that donor milk would  
384 be less effective. Holder pasteurization also negatively affects other antibacterial  
385 proteins such as Lactoferrin, which could also reduce donor milk's effectiveness (He et  
386 al., 2018; Pammi and Suresh, 2017). However, there are mitigating factors that might  
387 lessen the effects of pasteurization. First, donor milk provided to Neonatal Intensive

388 Care Units is often a mixture of multiple donors, which almost certainly broadens the  
389 anti-bacterial reactivity, which could be beneficial. Second, we don't actually know what  
390 the minimum functional amount of IgA binding to bacteria that is required to modulate  
391 intestinal colonization, partially because we do not fully understand the mechanism by  
392 which BrmIgA functions (Hand and Reboldi, 2021; Pabst and Slack, 2020; Yang and  
393 Palm, 2020). Finally, Human Milk Oligosaccharides, which shift the neonatal microbiota  
394 by increasing *Bifidobacteria*, are almost completely unaffected by pasteurization and  
395 very likely contribute to both preventing NEC and promoting a healthy infant microbiota  
396 (Bode, 2018).

397

398 Taken altogether we have demonstrated that there is substantial heterogeneity in the  
399 anti-bacterial reactivity of breast milk-derived IgA. We contend that this knowledge will  
400 serve as an important starting point for future studies on how binding by BrmIgA (or lack  
401 thereof) of newly colonizing bacteria shapes their ability to invade the infant intestine.

402

403 **Materials and Methods:**

404 Study Design:

405 *Research objectives:* Our objective was to identify the heterogeneity (or lack thereof) of  
406 breast milk derived IgA in response to common bacteria that colonize infants early after  
407 birth (in particular preterm infants).

408

409 *Research subjects:* De-identified milk donors from the Mid Atlantic Mother's Milk bank  
410 (Pittsburgh, PA) and or Mommy's Milk Human Milk Research Biorepository (San Diego,  
411 CA).

412

413 *Experimental Design:* We analyzed the anti-bacterial IgA reactivity with a custom  
414 bacterial flow cytometric array which we designed in our lab laboratory specifically for  
415 this purpose and is described in detail in both Figure 1 and below in the methods  
416 section. No randomization or blinding was used for this study.

417

418 *Sample size:* Since this was a discovery project and we really did not know the level of  
419 heterogeneity present within the breast milk-derived anti-bacterial IgA reactivity we did  
420 not perform a power analysis.

421

422 *Data inclusion and exclusion:* All samples that we acquired were analyzed, except  
423 samples where the IgA concentration was too low. In some cases, specific wells were  
424 omitted from our analysis if the number of bacteria in the well was insufficient for

425 analysis (mostly *M. nonliquefaciens*). No outliers were excluded. All acquired data is  
426 included in our analyses.

427

428 *Replicates:* Samples were processed and analyzed over many weeks and consistent  
429 flow cytometric measurements (though heterogeneous between samples) were an  
430 important internal control that was continuously assessed. During the development of  
431 our methodology we repeated IgA/bacterial binding assays on consecutive days with  
432 the same milk-derived IgA samples and bacterial isolates to confirm that the staining  
433 was repeatable.

434

435

436 *Samples and Protocols:*

437 *Human Donor Milk Samples*

438 The human study protocol was deemed ‘Not Human Research’ by the Institutional  
439 Review Board (Protocol number PRO19110221) of the University of Pittsburgh. The  
440 majority of the de-identified donor maternal milk was acquired from the Mid-Atlantic  
441 Mothers Milk Bank DBA Human Milk Science Institute and Biobank of Pittsburgh,  
442 Pennsylvania. We acquired de-identified maternal milk collected over multiple  
443 childbirths (dyads) from Mommy's Milk Human Milk Research Biorepository of San  
444 Diego, California. All donor milk samples were stored at -80° C.

445

446 *Donor metadata*

Cohort	Term (PA)	Preterm (PA)	Longitudinal (PA)	Two infants (CA)	Pasteurization
--------	-----------	--------------	-------------------	------------------	----------------

					<b>(PA)</b>
<b>Donor age (Years)</b>	32.5+/-4.2 (29-40) (unknown for 11 donors)	32.5+/-4.5 (19-38)	33.7+/-4.3 (29-40) (unknown for 1 donor)	31.7+/-3.9 (22-39) (includes age at 1 <sup>st</sup> and 2 <sup>nd</sup> infant)	30.5+/-8.3 (19-39)
<b>Est. Gest. age of infant at delivery (Weeks)</b>	39.6+/-+1.1 (37-41)	30.7+/-3.1 (25-35)	37.9+/-3.4 (32-41)	38.2+/-3.4 (25-42) (includes both infants)	36.5+/-4.4 (30-39)
<b>Time post-delivery of sample collection (Days)</b>	74.9+/-79.6 (14-276)	55.6+/-100.3 (4-330)	18+/-11.2 (3-42)	258.3+/-157.6 (44-688) (includes both infants)	7.5+/-1 (7-9)
<b>Race of donor</b>	100% Caucasian	93% Caucasian 7% Black	100% Caucasian	20% Caucasian 40% Black 40% Asian	100% Caucasian
<b>Ethnicity of donor</b>	Unknown	Unknown	Unknown	40% Hispanic	Unknown

447 Errors (+/-) represent the Standard Deviation. Number in brackets indicate range.

448 Metadata was not collected from all donors, as indicated. (PA = samples from

449 Pittsburgh, PA; CA = samples from San Diego, CA)

450

#### 451 *Immunoglobulin A Extraction*

452 To extract the IgA from milk, the donor milk was thawed at 4°C and 2mL of the maternal

453 milk was placed in a 2ml Eppendorf tube. To separate the whey protein from the fat, the

454 maternal milk was centrifuged at 16,000g for 5 mins at 4°C. The fat formed a layer at

455 the top of the tube and the cells at the bottom of the tube. The whey protein was

456 separated from the fat by carefully pipetting and filtering through a 0.22µm syringe filter,

457 followed by washing the 0.22µm syringe filter with 500µL of wash buffer [Phosphate

458 Buffered Saline (PBS)]. The filtered sample was then passed through a gravity flow

459 column containing peptide M agarose after equilibrating the column with PBS. The  
460 sample was allowed to completely enter the matrix. The columns were washed with  
461 20ml of 1X PBS. The column was then eluted with 10 mL elution buffer (0.1 M glycine,  
462 pH 2-3). 10ml of 1 M Tris with pH of 7.5 was used to neutralize the solution. The 20 mL  
463 sample was concentrated using a protein concentrator , by centrifugation of the column  
464 at 3000g for 20 min at 4° C. The concentrated sample was collected in 1.5 mL  
465 Eppendorf tubes and stored at -80° C.

466

#### 467 *Immunoglobulin A Quantification*

468 Prior to running IgA samples on our array protein content was estimated via  
469 measurement on a Nanodrop UV Spectrophotometer. The concentration of IgA in each  
470 sample was measured by ELISA (Abcam) according to the manufacturer's directions.

471

#### 472 *Protein separation and detection*

473 Various fractions of either protein (pre and post-Peptide M column) were loaded onto a  
474 gradient acrylamide gel (4-15 %) and separated by LDS-page electrophoresis prior to  
475 staining with Coomassie Blue stain. Alternatively, proteins separated by weight were  
476 transferred onto nitrocellulose membranes and identified by Western Blotting.

477 Membrane blocking and primary antibody staining was performed in TBS-Tween (X%)  
478 with the addition of powdered milk (anti-IgA Heavy Chain 1:10,000, Abcam; anti-Light  
479 Chain (kappa) 1:1000, Abcam; anti- J chain 1:500, ThermoFisher; anti-Secretory Factor  
480 1:400, Abcam)

481

482 *Bacterial Cultures and Flow cytometric Array development*

483 We identified 13 genera commonly found within preterm infants and identified strains  
484 within the University of Pittsburgh community and ATCC collection that would be  
485 representative of the preterm infant microbiota. Bacteria were grown according to  
486 guidelines provided by ATCC or the providing investigator (see chart below),  
487 approximately 18-42 hours. The bacteria were diluted two-fold (1:2) to measure OD.  
488 1mL of bacterial stock was then added to 1.5 mL eppendorf tube. The Eppendorf tube  
489 was centrifuged at 8,000g for 5 minutes and washed with 1 mL sterile 1X PBS twice.  
490 The supernatant was removed and re-suspended with 1 mL of sterile 1X PBS. The  
491 bacteria was then diluted to make the final concentration of  $8 \times 10^7$ /mL Colony Forming  
492 Units (CFU). To preserve the integrity of the bacteria during freezing process 100 $\mu$ L of  
493 glycerol was added to the dilution (1:10). 27 $\mu$ L of the bacteria and glycerol mixture was  
494 then added to 2 wells each in a 96-well U-bottom plate, as experiment and control. The  
495 plates (containing 36 samples) plates are then stored at -80° C.  
496

<b>Bacterial Isolate</b>	<b>Source</b>	<b>Growth Media</b>
<i>Citrobacter rodentium</i> 51459	American Type Culture Collection (ATCC)	Luria Bertani (LB) broth
<i>Enterobacter aerogenes</i> K457	R. Kowalski (University of Pittsburgh; PITT)	LB
<i>Enterobacter cloacae</i> K1535	R. Kowalski PITT	LB
<i>Escherichia coli</i> ( <i>E. coli</i> ) 587	L. Harrison/J. March PITT	LB
<i>E. coli</i> 596	L. Harrison/J. March PITT	LB
<i>E. coli</i> 605	L. Harrison/J.	LB



	March PITT	
<i>E. coli</i> 909 (K746)	R. Shanks PITT	LB
<i>E. coli</i> 910 (K1671)	R. Shanks PITT	LB
<i>E. coli</i> 4185 (EC100D)	R. Shanks PITT	LB
<i>E. coli</i> 2A	R. Longman (Weill Cornell)	LB
<i>E. coli</i> ECMB	Y. Belkaid (NIH); Hand (PITT)	LB
<i>E. coli</i> ECT5	Y. Belkaid (NIH); Hand (PITT)	LB
<i>E. coli</i> CUMT8	K. Simpson (Cornell University)	LB
<i>S. typhimurium</i> (SL3261)	Y. Belkaid (NIH); Hand (PITT)	LB
<i>Enterobacter spp.</i> (NEC)	M. Good (UNC SofM)	LB
<i>K. aerogenes</i> 13048	ATCC	LB
<i>K. oxytoca</i> 43165	ATCC	LB
<i>K. oxytoca</i> K405	R. Kowalski PITT	LB
<i>K. pneumoniae</i>	Y. Belkaid (NIH); Hand (PITT)	Tryptic Soy Broth (TSB)
<i>Serratia marcesens</i> 855	R. Shanks PITT	LB
<i>Serratia marcesens</i> 853	R. Shanks PITT	LB
<i>Proteus mirabilis</i>	R. Kowalski PITT	LB
<i>Proteus vulgaris</i>	R. Kowalski PITT	LB
<i>Pseudomonas</i> <i>aeruginosa</i> 01	Y. Belkaid (NIH); Hand (PITT)	LB
<i>Moraxella</i> <i>nonliquefaciens</i> E542	R. Kowalski PITT	LB
<i>Lactobacillus casei</i> 39539	ATCC	Lactobacilli MRS Broth
<i>Streptococcus</i> <i>agalactiae</i> BAA-2675	ATCC	Brain Heart Infusion Broth (BIH)
<i>Staphylococcus</i>	Y. Belkaid	TSB

<i>aureus</i> CT1	(NIH); Hand (PITT)	
<i>Staphylococcus capitis</i> 1931 (B1379)	R. Shanks PITT	LB
<i>Staphylococcus epidermidis</i> NIHLM087	Y. Belkaid (NIH)	Todd Hewitt Broth
<i>Staphylococcus epidermidis</i> NIHLM088	Y. Belkaid (NIH)	Todd Hewitt Broth
<i>Staphylococcus epidermidis</i> 247 (NARSA101)	R. Shanks PITT	LB
<i>Staphylococcus saprophyticus</i> 481 (E751)	R. Shanks PITT	LB
<i>Enterococcus faecalis</i> 2649 (E286)	R. Shanks PITT	LB
<i>Enterococcus faecalis</i> 19433	ATCC	BHI
<i>Enterococcus faecium</i> BAA-2946	ATCC	Lactobacilli MRS Broth
<i>Bradyrhizobium japonicum</i>	ATCC	Yeast Mannitol Broth

497

498 *Bacterial Flow Assay*

499 The bacterial plates, stored at -80°C were thawed at room temperature and washed  
500 twice (Swinging bucket centrifuge: 4,000 RPM for 5 minutes) with 200µL wash buffer  
501 [0.5% Bovine Serum Albumin (Sigma) in PBS-filtered through a 2.2µm filter]. The  
502 concentrated IgA from breast milk samples was thawed at 4°C and normalized to  
503 0.1mg/ml by diluting the sample with sterile PBS. 25µL of the normalized IgA with 25µL  
504 of sterile 1X PBS was added to all the bacteria in the experimental wells. For controls,  
505 50µL of sterile PBS was added. The plate was incubated for one hour in the dark on ice.  
506 After incubation, the plate was washed twice with 200µL wash buffer (4,000 RPM for 5  
507 minutes). All the wells in the 96-well plate were then stained with 50µL secondary

508 antibody staining mixture of Syto BC [(Green Fluorescent nuclear acid stain, Life  
509 Technologies (1:400)], APC Anti-Human IgA [Anti-Human IgA APC (Miltenyi Biotec  
510 clone REA1014, (1:50)], and blocking buffer of Normal Mouse Serum [ThermoFisher  
511 (1:10)]. The stained samples were incubated in the dark for an hour on ice. Samples  
512 were then washed three times with 200 $\mu$ L of wash buffer before flow cytometry analysis  
513 on the LSRFortessa-BD Biosciences.

514

515 For every donor we ran a separate plate that was stained only with the Syto BC/ APC  
516 anti-human IgA mix. These control samples are used as background fluorescence  
517 controls to establish positive binding signals and normalize samples collected on  
518 different days.

519

520

## 521 **Quantification and Statistical Analysis**

### 522 *Flow Cytometry*

523 All the data from flow cytometry was collected on a LSR Fortessa flow cytometer from  
524 BD Biosciences. The raw data was analyzed through the software FlowJo V10.4.2  
525 (FlowJo, OR, USA). All samples were normalized according to the following formula:  
526  $\text{Log}_2 \left[ \frac{\text{Geometric mean fluorescence intensity (gMFI) breast milk-derived IgA stained}}{\text{sample/ (gMFI of bacteria stained only with anti-human IgA APC antibody)}} \right]$ . Negative  
527 values (where the control has greater fluorescence than stained) are set to zero.  
528

529

### 530 *Principal Component Analysis*

531 Principal Component Analysis (PCA) plots were made using available R packages  
532 (ggplot2) and displays similarities in the percent binding of each donor sample to each  
533 bacterial taxon. Confidence ellipses demonstrate distinct groups based on multivariate t  
534 distribution.

535

#### 536 *Correlation Network Analyses*

537 We computed and visualized all pairwise Pearson correlations (of IgA binding profiles  
538 across bacterial isolates) in a heatmap using R. Significant correlations were defined  
539 using an effect size threshold of  $|r| > 0.7$  and an FDR ( $P$  value adjusted for multiple  
540 comparisons using Benjamini-Hochberg multiple testing correction) threshold of  $< 0.05$ .  
541 The significant correlations were visualized as a network using Cytoscape.

542

#### 543 *Statistical Tests and analysis software*

544 Heat maps were created using the MORPHEUS software tool (Broad Institute,  
545 Cambridge, MA). Hierarchical clustering by Spearman correlation. Samples collected  
546 over multiple infants were compared by either a standard or paired Student's t-test  
547 (GraphPad PRISM 9).

548

549

550 **Summary of supplemental material:** Three supplemental figures. Fig. S1 describes  
551 experiments related to the purification and quality control of IgA isolated from breast  
552 milk. Fig. S2 indicates the heterogeneity in BrmIgA anti-bacterial responses from

553 longitudinally collected samples. Fig. S3 displays paired analysis of infant dyads who  
554 share a mother where we collected milk samples used to feed both infants.

555

556

## 557 **Acknowledgements**

558 We would like to stress that we are only measuring the anti-bacterial IgA reactivity of  
559 breast milk samples and are not drawing conclusions on the best feeding option for any  
560 given infant. We would like to thank C. Verardi, D. O'Connor, K. Baumgartel and the  
561 entire staff of the Mid Atlantic Mother's Milk Bank (Pittsburgh). We would also like to  
562 thank K. Bertrand and C. Chambers and the Mommy's Milk Human Milk Research  
563 Biorepository of San Diego, California (UCSD). We would like to thank L. Harrison, R.  
564 Kowalski, J. Marsh, M. Morowitz and R. Shanks (Univ. of Pittsburgh, Pittsburgh, PA), R.  
565 Longman (Weill Cornell Medical School, New York, NY), Y. Belkaid (National Institutes  
566 of Health, Bethesda, MD), M. Good (University of North Carolina School of Medicine,  
567 Chapel Hill, NC) and K. Simpson (Cornell University, Ithaca, NY) for kindly providing  
568 bacterial strains and advice on strain selection. We would like to thank J. Michel and the  
569 Rangos Research Center Flow Cytometry core for assistance with running bacterial  
570 samples by flow cytometry. We would like to thank L. Cavacini for the anti-HIV IgA  
571 antibody. This work was supported by the UPMC Children's Hospital of Pittsburgh/R.K.  
572 Mellon Institute for Pediatric Research, the NIH (R01DK120697 to T.W.H. and  
573 T32AI089443 to A.H.P.B.) and a March of Dimes Innovative Challenge Grant (T.W.H.).  
574 T.W.H. and K.P.G. have a patent for the technology used for the identification of anti-  
575 bacterial antibodies from breast milk samples (US17/341,272). T.W.H. has been

576 engaged by Keller Postman LLC for his expertise on the components of breast milk that  
577 regulate intestinal colonization by bacteria and the development of Necrotizing  
578 Enterocolitis.

579

580 **Author contributions:** C.B. Johnson-Hence, K. P. Gopalakrishna, K.E. Coffey, D.  
581 Bodkin and T.W. Hand conceptualized the project, developed the methodology and  
582 designed the experiments. C.B. Johnson-Hence, K. P. Gopalakrishna, K.E. Coffey,  
583 Y.A. Sosa, D. Bodkin, D.A. Abbott, A.T. Rai and J.T. Tometich performed the  
584 experiments. C.B. Johnson-Hence, D. Bodkin, A.H.P. Burr, S. Rahman, J. Das and  
585 T.W. Hand analyzed the data. C.B. Johnson-Hence and T. W. Hand wrote the  
586 manuscript.

587

588

## 589 References

- 590 Ackerman, M.E., J. Das, S. Pittala, T. Broge, C. Linde, T.J. Suscovich, E.P. Brown, T.  
591 Bradley, H. Natarajan, S. Lin, J.K. Sassic, S. O'Keefe, N. Mehta, D. Goodman,  
592 M. Sips, J.A. Weiner, G.D. Tomaras, B.F. Haynes, D.A. Lauffenburger, C. Bailey-  
593 Kellogg, M. Roederer, and G. Alter. 2018. Route of immunization defines multiple  
594 mechanisms of vaccine-mediated protection against SIV. *Nat Med* 24:1590-1598.
- 595 Adhisivam, B., B. Vishnu Bhat, K. Rao, S.M. Kingsley, N. Plakkal, and C. Palanivel.  
596 2018. Effect of Holder pasteurization on macronutrients and immunoglobulin  
597 profile of pooled donor human milk. *J Matern Fetal Neonatal Med* 1-4.
- 598 Bemark, M., H. Hazanov, A. Stromberg, R. Komban, J. Holmqvist, S. Koster, J.  
599 Mattsson, P. Sikora, R. Mehr, and N.Y. Lycke. 2016. Limited clonal relatedness  
600 between gut IgA plasma cells and memory B cells after oral immunization. *Nat*  
601 *Commun* 7:12698.
- 602 Bode, L. 2018. Human Milk Oligosaccharides in the Prevention of Necrotizing  
603 Enterocolitis: A Journey From in vitro and in vivo Models to Mother-Infant Cohort  
604 Studies. *Front Pediatr* 6:385.
- 605 Bondt, A., K.A. Dingess, M. Hoek, D.M.H. van Rijswijck, and A.J.R. Heck. 2021. A  
606 Direct MS-Based Approach to Profile Human Milk Secretory Immunoglobulin A  
607 (IgA1) Reveals Donor-Specific Clonal Repertoires With High Longitudinal  
608 Stability. *Front Immunol* 12:789748.
- 609 Boyd, C.A., M.A. Quigley, and P. Brocklehurst. 2007. Donor breast milk versus infant  
610 formula for preterm infants: systematic review and meta-analysis. *Arch Dis Child*  
611 *Fetal Neonatal Ed* 92:F169-175.
- 612 Bunker, J.J., S.A. Erickson, T.M. Flynn, C. Henry, J.C. Koval, M. Meisel, B. Jabri, D.A.  
613 Antonopoulos, P.C. Wilson, and A. Bendelac. 2017. Natural polyreactive IgA  
614 antibodies coat the intestinal microbiota. *Science* 358:
- 615 Canizo Vazquez, D., S. Salas Garcia, M. Izquierdo Renau, and I. Iglesias-Platas. 2019.  
616 Availability of Donor Milk for Very Preterm Infants Decreased the Risk of  
617 Necrotizing Enterocolitis without Adversely Impacting Growth or Rates of  
618 Breastfeeding. *Nutrients* 11:
- 619 Cortez, J., K. Makker, D.F. Kraemer, J. Neu, R. Sharma, and M.L. Hudak. 2018.  
620 Maternal milk feedings reduce sepsis, necrotizing enterocolitis and improve  
621 outcomes of premature infants. *J Perinatol* 38:71-74.
- 622 Dixon, D.L. 2015. The Role of Human Milk Immunomodulators in Protecting Against  
623 Viral Bronchiolitis and Development of Chronic Wheezing Illness. *Children*  
624 *(Basel)* 2:289-304.
- 625 Flannery, D.D., E.M. Edwards, K.M. Puopolo, and J.D. Horbar. 2021. Early-Onset  
626 Sepsis Among Very Preterm Infants. *Pediatrics* 148:
- 627 Gopalakrishna, K.P., and T.W. Hand. 2020. Influence of Maternal Milk on the Neonatal  
628 Intestinal Microbiome. *Nutrients* 12:
- 629 Gopalakrishna, K.P., B.R. Macadangdang, M.B. Rogers, J.T. Tometich, B.A. Firek, R.  
630 Baker, J. Ji, A.H.P. Burr, C. Ma, M. Good, M.J. Morowitz, and T.W. Hand. 2019.  
631 Maternal IgA protects against the development of necrotizing enterocolitis in  
632 preterm infants. *Nat Med* 25:1110-1115.
- 633 Haas, A., K. Zimmermann, F. Graw, E. Slack, P. Rusert, B. Ledergerber, W. Bossart, R.  
634 Weber, M.C. Thurnheer, M. Battegay, B. Hirschel, P. Vernazza, N. Patuto, A.J.



- 635 Macpherson, H.F. Gunthard, and A. Oxenius. 2011. Systemic antibody  
636 responses to gut commensal bacteria during chronic HIV-1 infection. *Gut*  
637 60:1506-1519.
- 638 Haiden, N., and E.E. Ziegler. 2016. Human Milk Banking. *Ann Nutr Metab* 69 Suppl 2:8-  
639 15.
- 640 Hand, T.W., and A. Reboldi. 2021. Production and Function of Immunoglobulin A. *Annu*  
641 *Rev Immunol* 39:695-718.
- 642 Hapfelmeier, S., M.A. Lawson, E. Slack, J.K. Kirundi, M. Stoel, M. Heikenwalder, J.  
643 Cahenzli, Y. Velykoredko, M.L. Balmer, K. Endt, M.B. Geuking, R. Curtiss, 3rd,  
644 K.D. McCoy, and A.J. Macpherson. 2010. Reversible microbial colonization of  
645 germ-free mice reveals the dynamics of IgA immune responses. *Science*  
646 328:1705-1709.
- 647 He, Y.M., X. Li, M. Perego, Y. Nefedova, A.V. Kossenkov, E.A. Jensen, V. Kagan, Y.F.  
648 Liu, S.Y. Fu, Q.J. Ye, Y.H. Zhou, L. Wei, D.I. Gabrilovich, and J. Zhou. 2018.  
649 Transitory presence of myeloid-derived suppressor cells in neonates is critical for  
650 control of inflammation. *Nat Med* 24:224-231.
- 651 Johansen, F.E., and C.S. Kaetzel. 2011. Regulation of the polymeric immunoglobulin  
652 receptor and IgA transport: new advances in environmental factors that stimulate  
653 pIgR expression and its role in mucosal immunity. *Mucosal Immunol* 4:598-602.
- 654 Koch, M.A., G.L. Reiner, K.A. Lugo, L.S. Kreuk, A.G. Stanbery, E. Ansaldo, T.D. Seher,  
655 W.B. Ludington, and G.M. Barton. 2016. Maternal IgG and IgA Antibodies  
656 Dampen Mucosal T Helper Cell Responses in Early Life. *Cell* 165:827-841.
- 657 Landsverk, O.J., O. Snir, R.B. Casado, L. Richter, J.E. Mold, P. Reu, R. Horneland, V.  
658 Paulsen, S. Yaqub, E.M. Aandahl, O.M. Oyen, H.S. Thorarensen, M. Salehpour,  
659 G. Possnert, J. Frisen, L.M. Sollid, E.S. Baekkevold, and F.L. Jahnsen. 2017.  
660 Antibody-secreting plasma cells persist for decades in human intestine. *J Exp*  
661 *Med* 214:309-317.
- 662 Langel, S.N., F.C. Paim, M.A. Alhamo, A. Buckley, A. Van Geelen, K.M. Lager, A.N.  
663 Vlasova, and L.J. Saif. 2019. Stage of Gestation at Porcine Epidemic Diarrhea  
664 Virus Infection of Pregnant Swine Impacts Maternal Immunity and Lactogenic  
665 Immune Protection of Neonatal Suckling Piglets. *Front Immunol* 10:727.
- 666 Le Doare, K., B. Holder, A. Bassett, and P.S. Pannaraj. 2018. Mother's Milk: A  
667 Purposeful Contribution to the Development of the Infant Microbiota and  
668 Immunity. *Front Immunol* 9:361.
- 669 Lima, H.K., M. Wagner-Gillespie, M.T. Perrin, and A.D. Fogleman. 2017. Bacteria and  
670 Bioactivity in Holder Pasteurized and Shelf-Stable Human Milk Products. *Curr*  
671 *Dev Nutr* 1:e001438.
- 672 Lin, Y.C., A. Salieb-Aouissi, and T.A. Hooven. 2022. Interpretable prediction of  
673 necrotizing enterocolitis from machine learning analysis of premature infant stool  
674 microbiota. *BMC Bioinformatics* 23:104.
- 675 Lindner, C., I. Thomsen, B. Wahl, M. Ugur, M.K. Sethi, M. Friedrichsen, A. Smoczek, S.  
676 Ott, U. Baumann, S. Suerbaum, S. Schreiber, A. Bleich, V. Gaboriau-Routhiau,  
677 N. Cerf-Bensussan, H. Hazanov, R. Mehr, P. Boysen, P. Rosenstiel, and O.  
678 Pabst. 2015. Diversification of memory B cells drives the continuous adaptation  
679 of secretory antibodies to gut microbiota. *Nat Immunol* 16:880-888.



- 680 Miller, J., E. Tonkin, R.A. Damarell, A.J. McPhee, M. Sukanuma, H. Sukanuma, P.F.  
681 Middleton, M. Makrides, and C.T. Collins. 2018. A Systematic Review and Meta-  
682 Analysis of Human Milk Feeding and Morbidity in Very Low Birth Weight Infants.  
683 *Nutrients* 10:
- 684 Mirpuri, J., M. Raetz, C.R. Sturge, C.L. Wilhelm, A. Benson, R.C. Savani, L.V. Hooper,  
685 and F. Yarovinsky. 2014. Proteobacteria-specific IgA regulates maturation of the  
686 intestinal microbiota. *Gut Microbes* 5:28-39.
- 687 Moor, K., J. Fadlallah, A. Toska, D. Sterlin, M.L. Balmer, A.J. Macpherson, G.  
688 Gorochoy, M. Larsen, and E. Slack. 2016. Analysis of bacterial-surface-specific  
689 antibodies in body fluids using bacterial flow cytometry. *Nat Protoc* 11:1531-  
690 1553.
- 691 Neu, J., and W.A. Walker. 2011. Necrotizing enterocolitis. *N Engl J Med* 364:255-264.
- 692 Nino, D.F., C.P. Sodhi, and D.J. Hackam. 2016. Necrotizing enterocolitis: new insights  
693 into pathogenesis and mechanisms. *Nat Rev Gastroenterol Hepatol* 13:590-600.
- 694 Oddy, W.H. 2017. Breastfeeding, Childhood Asthma, and Allergic Disease. *Ann Nutr*  
695 *Metab* 70 Suppl 2:26-36.
- 696 Olm, M.R., N. Bhattacharya, A. Crits-Christoph, B.A. Firek, R. Baker, Y.S. Song, M.J.  
697 Morowitz, and J.F. Banfield. 2019. Necrotizing enterocolitis is preceded by  
698 increased gut bacterial replication, Klebsiella, and fimbriae-encoding bacteria. *Sci*  
699 *Adv* 5:eaax5727.
- 700 Pabst, O., and E. Slack. 2020. IgA and the intestinal microbiota: the importance of being  
701 specific. *Mucosal Immunol* 13:12-21.
- 702 Pammi, M., J. Cope, P.I. Tarr, B.B. Warner, A.L. Morrow, V. Mai, K.E. Gregory, J.S.  
703 Kroll, V. McMurtry, M.J. Ferris, L. Engstrand, H.E. Lilja, E.B. Hollister, J.  
704 Versalovic, and J. Neu. 2017. Intestinal dysbiosis in preterm infants preceding  
705 necrotizing enterocolitis: a systematic review and meta-analysis. *Microbiome*  
706 5:31.
- 707 Pammi, M., and G. Suresh. 2017. Enteral lactoferrin supplementation for prevention of  
708 sepsis and necrotizing enterocolitis in preterm infants. *Cochrane Database Syst*  
709 *Rev* 6:CD007137.
- 710 Peila, C., G.E. Moro, E. Bertino, L. Cavallarin, M. Giribaldi, F. Giuliani, F. Cresi, and A.  
711 Coscia. 2016. The Effect of Holder Pasteurization on Nutrients and Biologically-  
712 Active Components in Donor Human Milk: A Review. *Nutrients* 8:
- 713 Planer, J.D., Y. Peng, A.L. Kau, L.V. Blanton, I.M. Ndao, P.I. Tarr, B.B. Warner, and J.I.  
714 Gordon. 2016. Development of the gut microbiota and mucosal IgA responses in  
715 twins and gnotobiotic mice. *Nature* 534:263-266.
- 716 Quigley, M., N.D. Embleton, and W. McGuire. 2018. Formula versus donor breast milk  
717 for feeding preterm or low birth weight infants. *Cochrane Database Syst Rev*  
718 6:CD002971.
- 719 Ramanan, D., E. Sefik, S. Galvan-Pena, M. Wu, L. Yang, Z. Yang, A. Kostic, T.V.  
720 Golovkina, D.L. Kasper, D. Mathis, and C. Benoist. 2020. An Immunologic Mode  
721 of Multigenerational Transmission Governs a Gut Treg Setpoint. *Cell* 181:1276-  
722 1290 e1213.
- 723 Reyman, M., M.A. van Houten, D. van Baarle, A. Bosch, W.H. Man, M. Chu, K. Arp,  
724 R.L. Watson, E.A.M. Sanders, S. Fuentes, and D. Bogaert. 2019. Impact of

- 725 delivery mode-associated gut microbiota dynamics on health in the first year of  
726 life. *Nat Commun* 10:4997.
- 727 Rogier, E.W., A.L. Frantz, M.E. Bruno, L. Wedlund, D.A. Cohen, A.J. Stromberg, and  
728 C.S. Kaetzel. 2014. Secretory antibodies in breast milk promote long-term  
729 intestinal homeostasis by regulating the gut microbiota and host gene  
730 expression. *Proc Natl Acad Sci U S A* 111:3074-3079.
- 731 Rognum, T.O., S. Thrane, L. Stoltenberg, A. Vege, and P. Brandtzaeg. 1992.  
732 Development of intestinal mucosal immunity in fetal life and the first postnatal  
733 months. *Pediatr Res* 32:145-149.
- 734 Rollenske, T., V. Szijarto, J. Lukasiewicz, L.M. Guachalla, K. Stojkovic, K. Hartl, L.  
735 Stulik, S. Kocher, F. Lasitschka, M. Al-Saeedi, J. Schroder-Braunstein, M. von  
736 Frankenberg, G. Gaebel, P. Hoffmann, S. Klein, K. Heeg, E. Nagy, G. Nagy,  
737 and H. Wardemann. 2018. Cross-specificity of protective human antibodies  
738 against *Klebsiella pneumoniae* LPS O-antigen. *Nat Immunol* 19:617-624.
- 739 Roux, M.E., M. McWilliams, J.M. Phillips-Quagliata, P. Weisz-Carrington, and M.E.  
740 Lamm. 1977. Origin of IgA-secreting plasma cells in the mammary gland. *J Exp*  
741 *Med* 146:1311-1322.
- 742 Sandin, C., S. Linse, T. Areschoug, J.M. Woof, J. Reinholdt, and G. Lindahl. 2002.  
743 Isolation and detection of human IgA using a streptococcal IgA-binding peptide. *J*  
744 *Immunol* 169:1357-1364.
- 745 Slack, E., S. Hapfelmeier, B. Stecher, Y. Velykoredko, M. Stoel, M.A. Lawson, M.B.  
746 Geuking, B. Beutler, T.F. Tedder, W.D. Hardt, P. Bercik, E.F. Verdu, K.D.  
747 McCoy, and A.J. Macpherson. 2009. Innate and adaptive immunity cooperate  
748 flexibly to maintain host-microbiota mutualism. *Science* 325:617-620.
- 749 Sobti, J., G.P. Mathur, A. Gupta, and Who. 2002. WHO's proposed global strategy for  
750 infant and young child feeding: a viewpoint. *J Indian Med Assoc* 100:502-504,  
751 506.
- 752 Suscovich, T.J., J.K. Fallon, J. Das, A.R. Demas, J. Crain, C.H. Linde, A. Michell, H.  
753 Natarajan, C. Arevalo, T. Broge, T. Linnekin, V. Kulkarni, R. Lu, M.D. Stein, C.  
754 Luedemann, M. Marquette, S. March, J. Weiner, S. Gregory, M. Coccia, Y.  
755 Flores-Garcia, F. Zavala, M.E. Ackerman, E. Bergmann-Leitner, J. Hendriks, J.  
756 Sadoff, S. Dutta, S.N. Bhatia, D.A. Lauffenburger, E. Jongert, U. Wille-Reece,  
757 and G. Alter. 2020. Mapping functional humoral correlates of protection against  
758 malaria challenge following RTS,S/AS01 vaccination. *Sci Transl Med* 12:  
759 Walker, W.A., and R.S. Iyengar. 2015. Breast milk, microbiota, and intestinal immune  
760 homeostasis. *Pediatr Res* 77:220-228.
- 761 Warner, B.B., and P.I. Tarr. 2016. Necrotizing enterocolitis and preterm infant gut  
762 bacteria. *Semin Fetal Neonatal Med* 21:394-399.
- 763 Wilson, E., and E.C. Butcher. 2004. CCL28 controls immunoglobulin (Ig)A plasma cell  
764 accumulation in the lactating mammary gland and IgA antibody transfer to the  
765 neonate. *J Exp Med* 200:805-809.
- 766 Yang, Y., and N.W. Palm. 2020. Immunoglobulin A and the microbiome. *Curr Opin*  
767 *Microbiol* 56:89-96.
- 768 Yu, X., M. Duval, C. Lewis, M.A. Gawron, R. Wang, M.R. Posner, and L.A. Cavacini.  
769 2013. Impact of IgA constant domain on HIV-1 neutralizing function of  
770 monoclonal antibody F425A1g8. *J Immunol* 190:205-210.

771 Zhang, W., Q. Feng, C. Wang, X. Zeng, Y. Du, L. Lin, J. Wu, L. Fu, K. Yang, X. Xu, H.  
772 Xu, Y. Zhao, X. Li, U.H. Schoenauer, A. Stadlmayr, N.K. Saksena, H. Tilg, C.  
773 Datz, and X. Liu. 2017. Characterization of the B Cell Receptor Repertoire in the  
774 Intestinal Mucosa and of Tumor-Infiltrating Lymphocytes in Colorectal Adenoma  
775 and Carcinoma. *J Immunol* 198:3719-3728.  
776 Zikan, J., J. Novotny, T.L. Trapane, M.E. Koshland, D.W. Urry, J.C. Bennett, and J.  
777 Mestecky. 1985. Secondary structure of the immunoglobulin J chain. *Proc Natl*  
778 *Acad Sci U S A* 82:5905-5909.  
779  
780  
781

782 **Figure Legends**

783 **Figure 1 – A flow cytometric array for measuring the anti-bacterial specificity of**  
784 **breast milk-derived IgA.**

785 **A)** Design of the flow cytometric array. Made with BioRender.com

786 **B)** Examples of SYTO BC<sup>+</sup>/SSC<sup>Dim</sup> staining used to discriminate bacteria from  
787 debris/bubbles in the flow cytometer (control is empty well stained with SYTO BC).  
788 Numbers represent the percent of events inside the gate.

789 **C)** Examples of the magnitude of anti-bacterial IgA binding detected in our array  
790 comparing two donors (9 and 10) that differ in their anti-bacterial IgA responses. The  
791 bottom row shows the reactivity of an anti-HIV IgA antibody against the same bacterial  
792 isolates. Numbers in red represent the gMFI of that sample.

793 **D)** Breast milk-derived IgA reactivity, from several donors (as indicated) against the  
794 environmental bacteria *Bradyrhizobium japonicum*.

795

796 **Figure 2 – Heterogeneity in the anti-bacterial reactivity of breast milk-derived IgA.**

797 Donor milk samples (term infants; >37 weeks gestational age) were analyzed with our  
798 flow cytometric array (**1A**).

799 **A)** Heat map of normalized anti-bacterial IgA binding affinity of different donors.  
800 Hierarchical clustering (Spearman). The range of the normalized values across each  
801 row is indicated on the left hand column.

802 **B)** Scatter graph showing the normalized anti-bacterial IgA binding values for each  
803 donor (each color represents a different donor).

804 **C)** Scatter graph of the normalized BrmIgA binding to different isolates of *E. coli*  
805 separated according to donors selected from the analysis in **(2A)**.  
806 **D-E)** A correlation network analysis was performed to describe which anti-bacterial IgA  
807 responses were predictive.  
808 **D)** Network diagram indicating significantly correlated anti-bacterial IgA responses.  
809 **E)** Heat map indicating the level of correlation between different bacteria in our array.  
810 Black box drawn around *Enterobacteriaceae* family taxa.

811

812 **Figure 3 – Heterogeneity in the breast milk-derived anti-bacterial IgA reactivity**  
813 **from donors who delivered preterm infants.**

814 Donor milk samples (preterm infants; 24-35 weeks gestational age) were analyzed with  
815 our flow cytometric array **(1A)**.

816 **A)** Bar graph showing the concentration of IgA purified from donor milk samples from  
817 mothers of term and preterm infants (ELISA).

818 **B)** Heat map of normalized anti-bacterial binding affinity of different preterm donors.  
819 (Spearman). Samples where no data was collected due to insufficient bacteria in the  
820 well are colored grey.

821 **C)** Scatter graph showing the normalized anti-bacterial IgA binding values for each  
822 preterm donor (each color represents a different donor).

823 **D)** Principal Component Analysis (PCA) comparing aggregate anti-bacterial IgA binding  
824 between preterm and term samples.

825

826 **Figure 4 - Temporal stability of anti-bacterial maternal IgA reactivity within one**  
827 **childbirth/infant.**

828 Multiple milk samples were collected from different donors over time and analyzed with  
829 our flow cytometric array (**1A**).

830 **A)** Heat map of normalized anti-bacterial binding affinity of different donors. Hierarchical  
831 clustering (Spearman) of various donors is indicated by colored bars above and below  
832 the heatmap. Date of collection indicated on heatmap: D##, where the number is days  
833 post-delivery)

834 **B)** Scatter graph showing the normalized anti-bacterial IgA binding values for each  
835 sample from longitudinally collected donors (each color represents a different donor;  
836 from **4A**).

837 **C-D)** PCA of the aggregate anti-bacterial IgA binding of longitudinally collected samples.  
838 Each donor colored as in **4A**.

839 **C)** PCA of individual longitudinally collected samples where symbols indicate the time of  
840 collection (week post delivery).

841 **D)** PCA from **C** where ellipses indicate the maximum variance for each donor cluster  
842 along each axis. No ellipses are drawn for samples where fewer than four samples were  
843 available.

844

845 **Figure 5 – Stability of the breast milk-derived anti-bacterial IgA reactivity through**  
846 **sibling infants.**

847 Breast milk samples were collected from consecutive siblings and analyzed with our  
848 flow cytometric array (**1A**).

849 **A)** Heat map of normalized anti-bacterial binding affinity of different donors. Hierarchical  
850 clustering (Spearman) of various donors is indicated by colored bars above and below  
851 the heatmap that correspond to each donor.

852 **B)** PCA of aggregate anti-bacterial samples where each donor is displayed in a different  
853 color (from **5A**). The first sibling is indicated by a circle and the second sibling a triangle.  
854 Samples colored as in **5A**.

855 **C)** Paired Student's t-tests were calculated comparing the IgA binding of each donor  
856 between infant one and infant two for each bacterial taxon. The mean change  $((\text{Infant 2}$   
857  $-\text{Infant 1; taxa 1}) + (\text{Infant 2} - \text{Infant 1; taxa x}))/37$  (#of taxa) for each paired test was  
858 calculated and graphed. Significant increase in 2<sup>nd</sup> infant = 'up' triangle; significant  
859 decrease in 2<sup>nd</sup> infant = 'down' triangle; no statistical significance = circle. Colors are  
860 according to **5A**. See Supplemental Figure 3 for each Paired Student's t test.

861

862 **Figure 6 – Holder pasteurization reduces the bacterial binding properties of**  
863 **breast milk-derived IgA**

864 Breast milk samples from four donors were split into two where one half was  
865 pasteurized (62.5°C for 30 minutes) while the other untreated as a control. IgA was then  
866 isolated from both halves and analyzed on our flow cytometric array (**1A**).

867 **A)** Paired Student's t-test ( $***p < 0.001$ ) of the IgA concentration (mg/mL) of control (blue)  
868 and pasteurized samples (red), as measured by ELISA .

869 **B)** Paired Student's t-tests comparing control (blue ) and Holder pasteurized (red) milk  
870 samples from the same donor. Each dot represents a different bacterial taxon.

871  $****p < 0.0001$ .



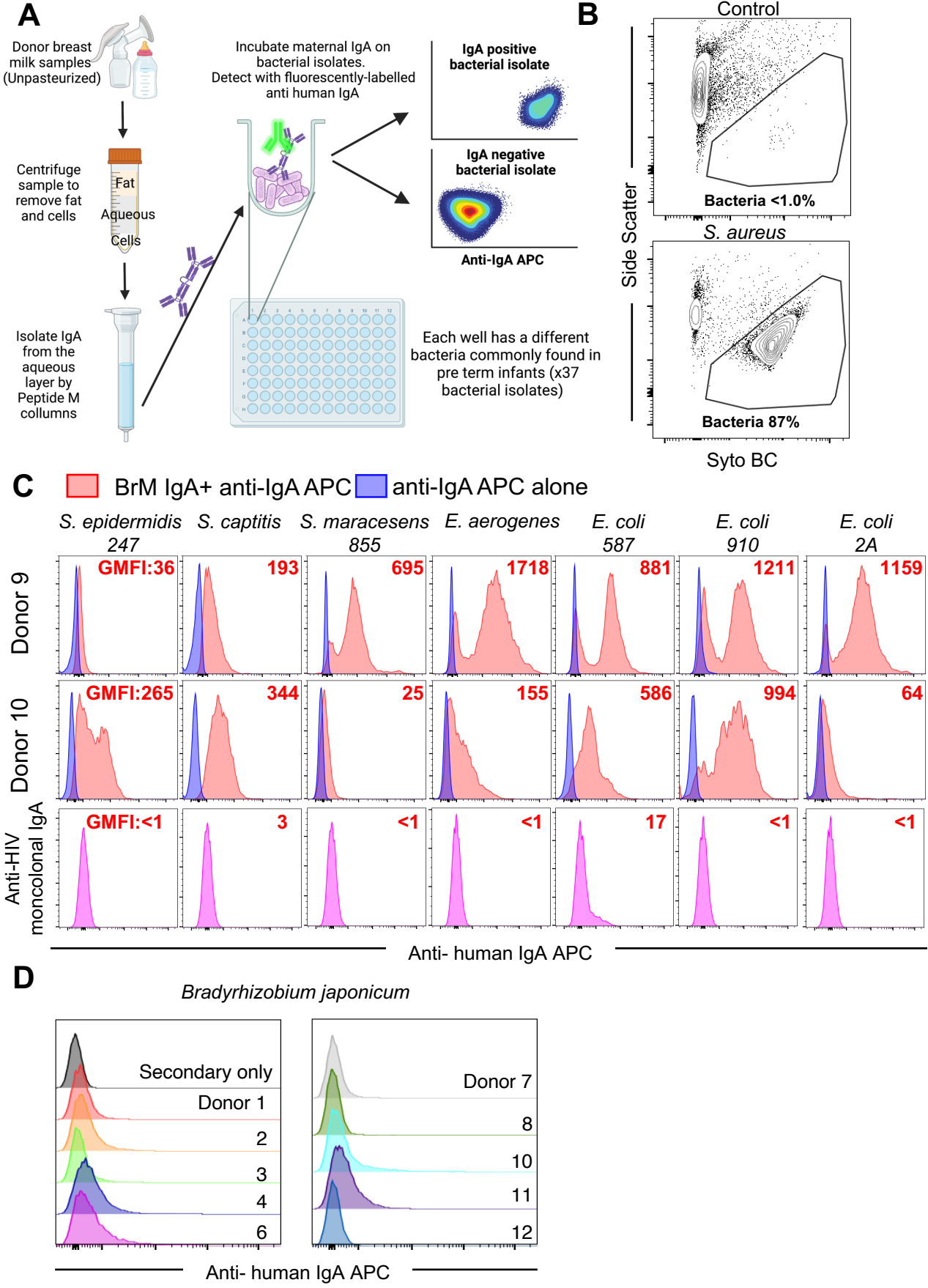


**Figure 1**



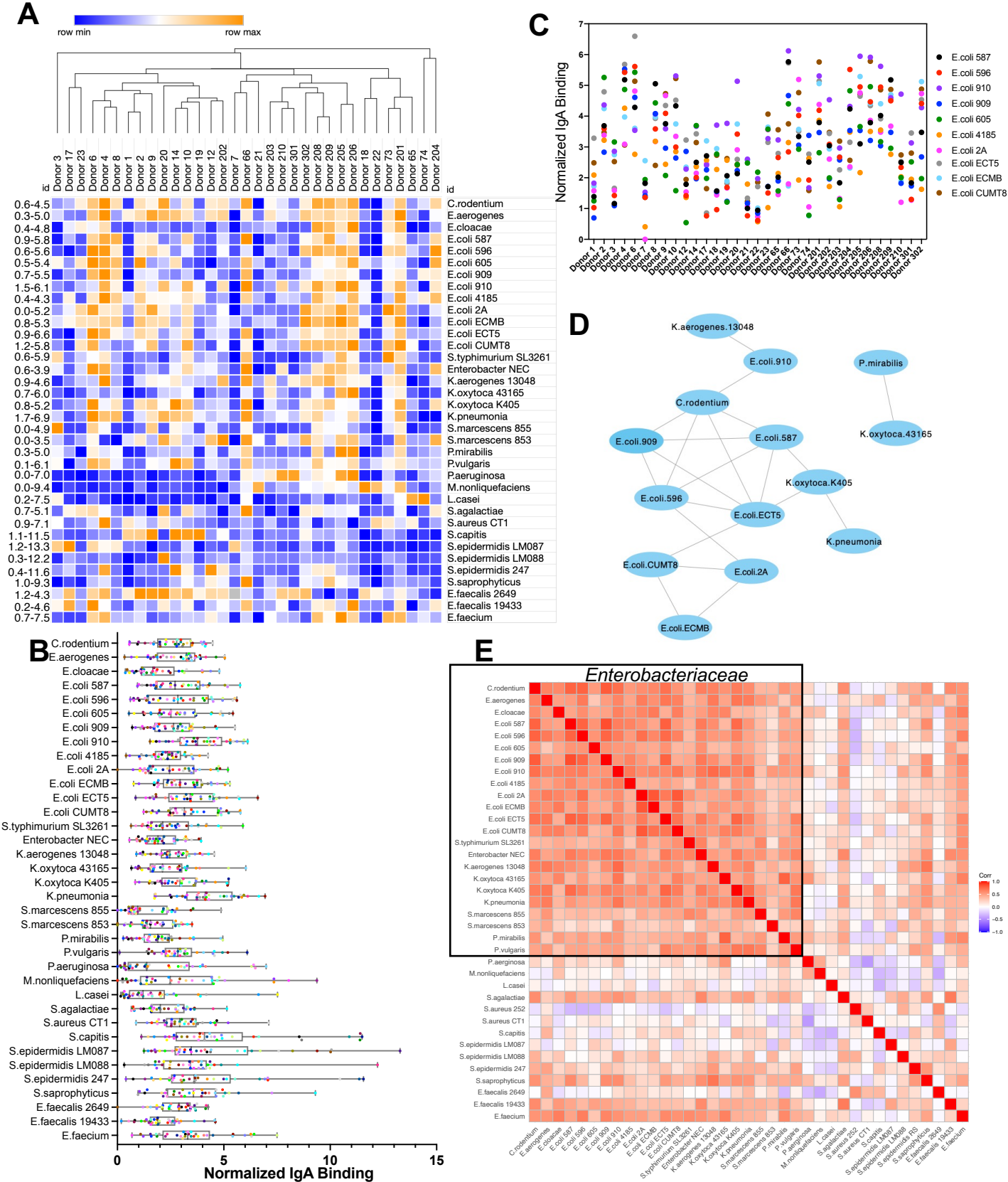


**Figure 2**

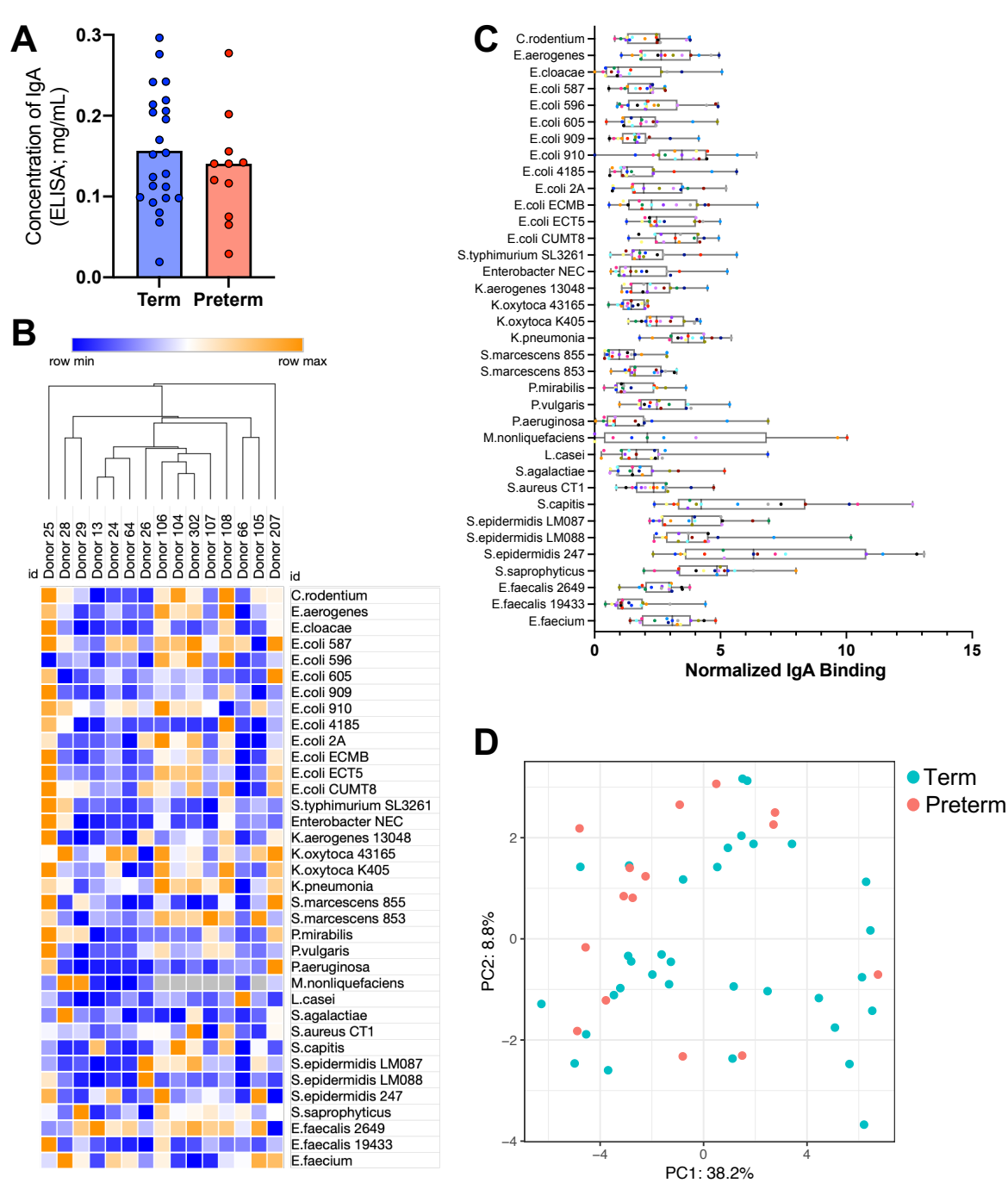


**Figure 3**

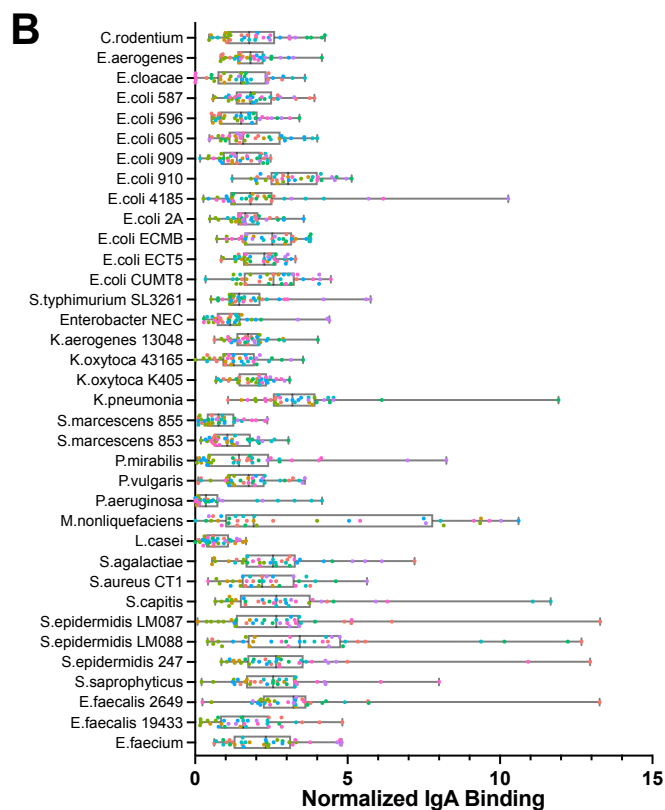
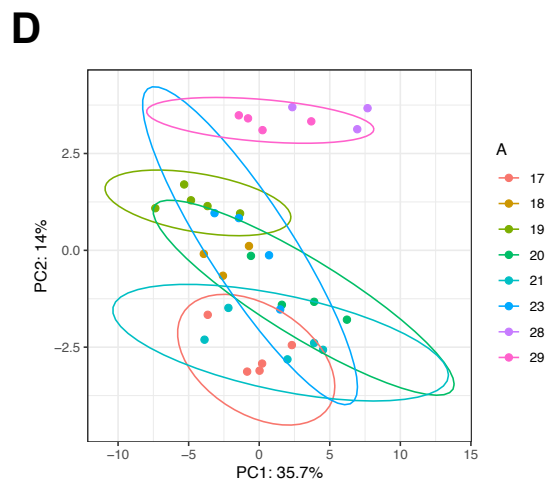
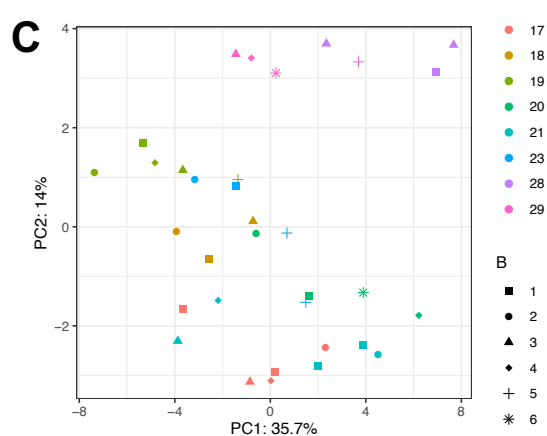
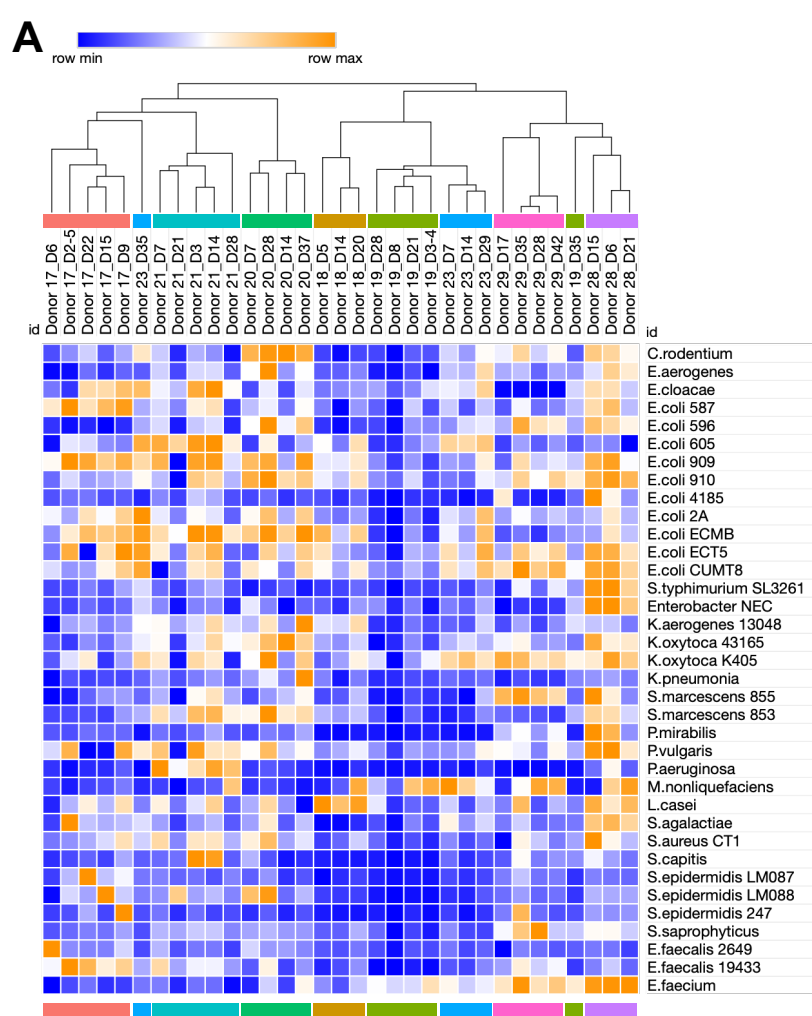


**Figure 4**

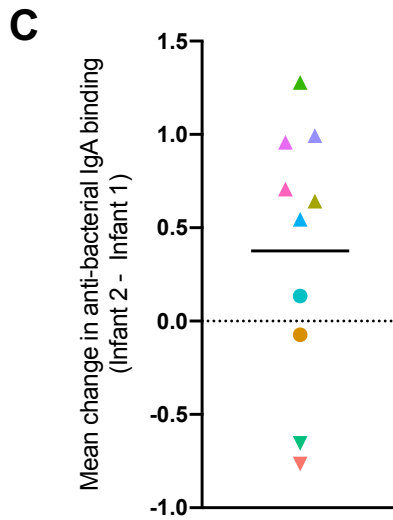
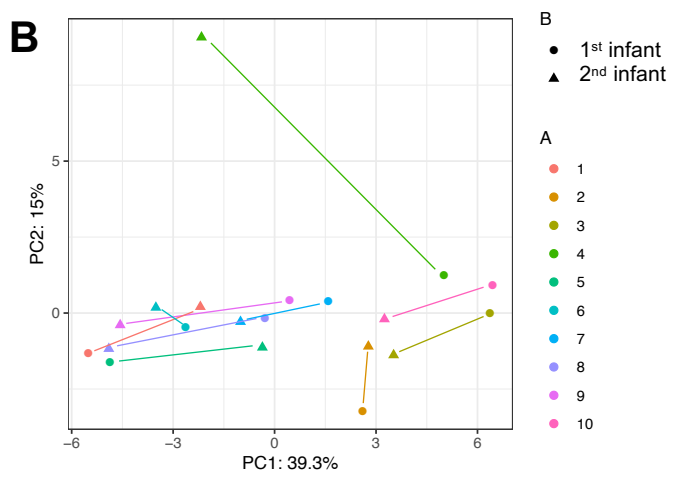
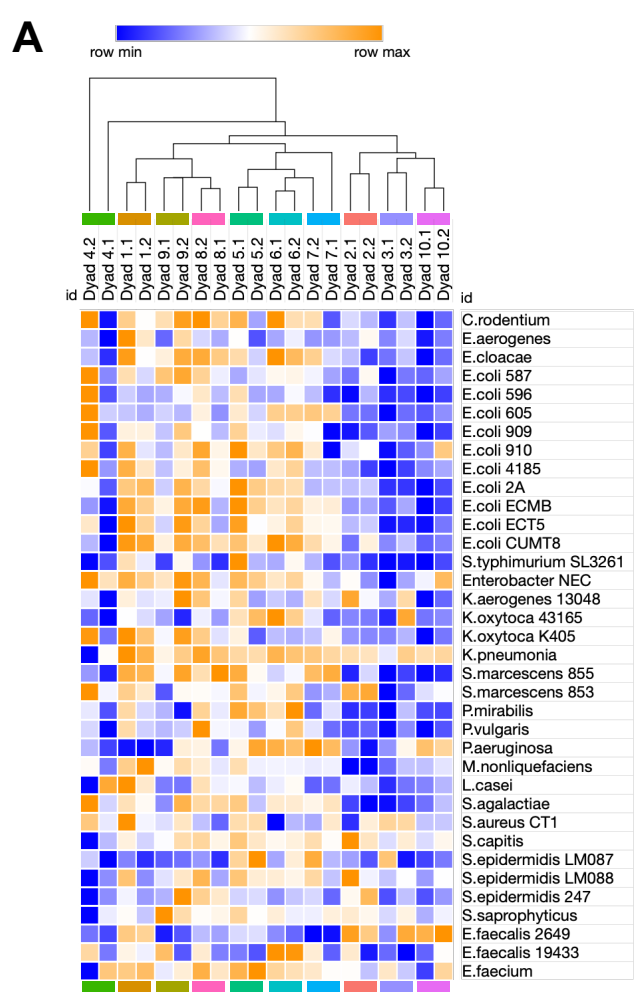


**Figure 5**

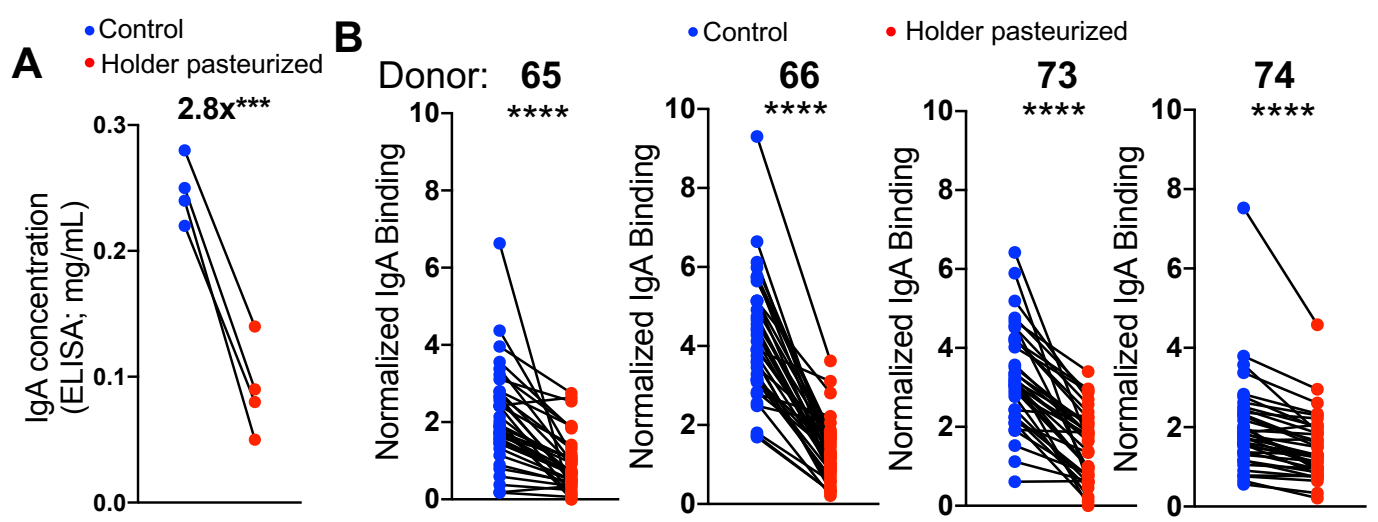


**Figure 6**